

Selective Modification of the Acid–Base Properties of Ceria by Supported Au

Manuela C. I. Bezen,^[a] Cornelia Breitkopf,^[a] Nadia El Kolli,^[b] Jean-Marc Krafft,^[b] Catherine Louis,^[b] and Johannes A. Lercher^{*,[a]}

Abstract: Au supported on CeO₂ prepared by deposition–precipitation with urea leads to a basic catalyst. Au acts in two ways as surface modifier. First, Au selectively interacts with Ce⁴⁺ cations by either blocking access to or reducing Ce⁴⁺ to Ce³⁺. Second, the resulting Au atoms (presumably as Au⁺ ions) act as soft, weak Lewis acid sites

stabilizing carbanion intermediates and enhancing hydride abstraction in the dehydrogenation of alcohols. In consequence, the thus-synthesized basic cata-

Keywords: cerium • gold • heterogeneous catalysis • IR spectroscopy • supported catalysts

lyst catalyzes the dehydrogenation of propan-2-ol to acetone with high efficiency and without notable deactivation. Additionally, the dehydration pathway of propan-2-ol is eliminated, as Au also quantitatively blocks access to strongly acidic Ce⁴⁺ ions or reduces them to Ce³⁺.

Introduction

Ceria is a material of high catalytic relevance and has therefore been extensively studied.^[1,2] For example, ceria is used as catalyst in alcohol conversion on the basis of its unique combination of acid–base properties.^[3] The redox properties of ceria make it an interesting support for gold catalysts.^[4] Gold supported on ceria has received particular attention due to its high activity at low temperatures for a number of reactions including oxidation of CO,^[5] preferential oxidation of CO in the presence of H₂,^[6] oxidation of unsaturated ketones,^[7] hydrogenation of nitro compounds,^[8] reduction of NO_x,^[9] and the low-temperature water-gas shift reaction.^[10–14] The unique properties of ceria-supported Au catalysts depend on a variety of factors, such as the dispersion of the nanoscale particles,^[15–17] the oxidation state of the Au particles,^[18] and the type of ceria used.^[19–21]

There is an on-going discussion about the nature of the active gold species in ceria-based catalysts. Several surface science and theoretical studies addressed in detail the nature and mechanism of Au on ceria. Density functional studies on CeO₂(111) slab models by Castellani et al.^[22] favored deposition of Au on oxygen atoms in different facets of ceria surfaces resulting in either neutral or oxidized Au species. Using STM and XPS studies on CeO₂(111) Baron et al.,^[23] on the other hand, argue that the concentration of

Ce⁴⁺ in nanostructured ceria thin films decreased after deposition of Au and observed simultaneously a significant concentration of oxidized Au species. The deposition of Au appears, therefore, to markedly alter the acid–base properties of ceria. In both cases, deposition of Au appears to either block or alter Lewis acid or base sites of model ceria surfaces, and this suggests a significant modification of its acid–base properties. Thus, we decided to explore whether Au can be used to selectively modify the acid–base properties of real powder ceria catalysts and whether such a modification would be sufficient to manifest itself in catalytic transformations.

While characterization of the acid properties is well established, characterization of the basic properties by probe molecules is not straightforward, because their application is limited to a certain range of base strength.^[24] Therefore, we decided to use the well-established probe reaction of conversion of propan-2-ol. Depending on the nature and strength of active sites, propan-2-ol is dehydrated to propene or diisopropyl ether on acidic sites,^[25,26] or dehydrogenated to acetone on predominantly basic sites.^[25,27,28,29] However, it was also claimed that redox properties play a role in propan-2-ol dehydrogenation.^[30] High-temperature calcination of ceria (above 800 °C), for example, decreased the strength of Lewis acid sites on the surface and enhanced the formation of basic sites suppressing propan-2-ol dehydration.^[31]

The main objective of the current study was therefore to explore the influence of Au on the acid–base properties of ceria. Acid–base properties and metal state were characterized by IR spectroscopy with adsorption of probe molecules such as pyridine and CO. The catalytic properties with regard to propan-2-ol conversion were followed in a flow reactor at different temperatures and for different activation procedures as well as by in situ IR spectroscopy during the reaction.

[a] M. C. I. Bezen, Dr. C. Breitkopf, Prof. Dr. J. A. Lercher
Department Chemie
Technische Universität München
Lichtenbergstr. 4, 85748 Garching (Germany)
Fax: (+49) 89-289-13544
E-mail: johannes.lercher@ch.tum.de

[b] N. El Kolli, J.-M. Krafft, Dr. C. Louis
Laboratoire de Réactivité de Surface, UMR 7197 CNRS
Université Pierre et Marie Curie, UPMC
4 place Jussieu, 75252 Paris cedex 05 (France)

Experimental Section

Materials: Commercial ceria with a specific surface area of approximately $6\text{ m}^2\text{ g}^{-1}$ was obtained from Merck and pretreated in synthetic air at 100 mL min^{-1} by increasing the temperature from ambient to 600°C with an increment of $10^\circ\text{C min}^{-1}$ for 8 h. The sample is referred to oxidized ceria. For comparison ceria was also pretreated under hydrogen atmosphere at 300°C (5°C min^{-1}) for 2 h. This sample is referred to reduced ceria.

The ceria-supported Au catalysts were prepared from oxidized ceria by the deposition-precipitation (DP) method with urea, as described previously by Delannoy et al.^[19] The Au precursor was generated by dissolving $\text{HAuCl}_4 \cdot 3\text{H}_2\text{O}$ (1 g, 2.54 mmol) in 100 mL of deionized water (0.0254 mol L^{-1}). The pretreated ceria (3 g) was suspended in 300 mL of water and heated at 80°C . Two Au loadings (0.1 and 1.0 wt %) were generated by adding the appropriate amount of the precursor solution followed by adding the related amount of urea immediately (see Table 1). The suspensions were stirred for 16 h at 80°C . Afterwards, the materials

Table 1. Characteristics of ceria and Au/CeO₂ samples: details of preparation, gold loadings, particle sizes, rates at 225°C to main products propene or acetone. Rates were measured at 225°C in a flow of 40 mL min^{-1} He saturated with propan-2-ol at 13°C .

| Sample | Au precursor [mL] | Urea addition [g] | Au loading [wt %] | Particle size [nm] | Rate to propene [$\mu\text{mol g}^{-1}\text{ s}^{-1}$] | Rate to acetone [$\mu\text{mol g}^{-1}\text{ s}^{-1}$] | Selectivity to acetone [%] |
|--|-------------------|-------------------|-------------------|--------------------|--|--|----------------------------|
| CeO ₂ (oxidized) ^[a] | – | – | – | – | 35 | 0.5 | 1 |
| CeO ₂ (reduced) ^[b] | – | – | – | – | 19 | 0 | 0 |
| Au/CeO ₂ (0.1) ^[b] | 0.6 | 0.09 | 0.16 | – | 0 | 308 | 100 |
| Au/CeO ₂ (1.0) ^[b] | 6.0 | 0.90 | 0.84 | 1.4 | 0 | 847 | 100 |

[a] The sample was pretreated at 500°C in He for 1 h. [b] The sample was pretreated at 500°C in H₂ for 1 h.

were washed with deionized water. Washing was repeated (with centrifugation after each washing step) until the pH of the solution was 7 and neither Au nor Cl[–] was detected by testing with NaBH₄ and AgNO₃, respectively. Both samples were dried in vacuum at ambient temperature for 16 h. Before use in IR characterization or reaction, the samples were reduced in H₂ at the given temperature. The samples are referred to Au/CeO₂(1.0) and Au/CeO₂(0.1).

Usually, thermal reduction or calcination treatments were performed from ambient temperature to 300°C (5°C min^{-1}) in a flow of 100 mL min^{-1} H₂ or synthetic air, and a plateau at 300°C was maintained for 2 h. The samples were cooled to room temperature in a flow of 100 mL min^{-1} He.

Characterization: Chemical analysis was performed by inductively coupled plasma emission spectroscopy at the CNRS Center of Chemical Analysis (Vernaison, France).

The specific surface areas and pore volumes were determined by physisorption of N₂ at 77 K. Measurements were carried out in a PMI automatic BET-Sorptometer. Evaluation was done according to the BET theory.

The crystalline structure was analyzed by XRD on a Philips X'Pert Pro System (Cu_{K α} radiation $\lambda = 0.154\text{ nm}$) at 40 kV/40 mA. Measurements were carried out on a spinner with a 1/6-inch slit in the range $2\theta = 20\text{--}70^\circ$ with a step size of $0.05^\circ\text{ min}^{-1}$.

For transmission electron microscopy (TEM), the sample was ground, suspended in ethanol, and ultrasonically dispersed. An appropriate amount of the as-prepared dispersion was dropped on a copper-grid supported carbon film. Micrographs were recorded on a JEM-2010 Jeol transmission microscope operating at 120 kV. The average metal particle sizes d_{Au} were determined from measurements on about 150 particles and were expressed as the arithmetic mean: $d_{\text{Au}} = \sum n_i d_i / \sum n_i$, where n_i is the number of particles of diameter d_i .

IR spectroscopy of adsorbed pyridine was carried out on a Thermo Nicolet spectrometer coupled with an MCT detector. For IR spectroscopic measurements in transmission mode, the samples were pressed into self-

supporting wafers and activated in situ at 300°C for 2 h in vacuum. The spectra were recorded in transmission mode at a resolution of 4 cm^{-1} over the wavenumber range $4000\text{--}800\text{ cm}^{-1}$. After recording the catalyst background spectrum, pyridine was adsorbed at 0.1 mbar and 50°C . Weakly adsorbed pyridine was removed by increasing the temperature from 50 to 200°C for 0.5 h in vacuum (10^{-5} mbar).

The IR spectra of adsorbed CO for the gold-containing samples were recorded in transmission mode at liquid-N₂ temperature by using a Bruker Vector 22 spectrometer with a spectral resolution of 2 cm^{-1} and accumulation of 64 scans. Self-supporting pellets were prepared from the as-prepared sample powders and treated in situ in the IR cell. The latter was connected to a vacuum-adsorption apparatus with a residual pressure below 10^{-6} mbar. Prior to the IR experiments, the samples were activated in hydrogen (100 mL min^{-1}) from RT to 300°C (2°C min^{-1}), maintained at that temperature for 2 h, and then evacuated for 30 min. The adsorption experiments were performed at liquid-nitrogen temperature to characterize specific adsorption sites on the metal as well as on metal oxides that interact weakly with CO.

The conversion of propan-2-ol was followed by IR spectroscopy in transmission mode on a Bruker IFS 88 spectrometer. The self-supporting pellets were heated in situ in a flow of 20 mL min^{-1} of synthetic air (oxidized ceria) or H₂ (reduced ceria and Au/ceria) from ambient temperature to 300°C (5°C min^{-1}), then at 300°C for 2 h, and were subsequently cooled to 150°C in a flow of 20 mL min^{-1} He. The spectra were recorded in transmission mode with a resolution of 4 cm^{-1} over the wavenumber range $4000\text{--}800\text{ cm}^{-1}$. After activation a background spectrum was taken at 150°C .

A flow of 10 mL min^{-1} He was saturated with propan-2-ol at 13°C ($p_{\text{propan-2-ol}} = 25\text{ mbar}$) and led over the sample. Spectra were recorded every 2 min for 10 min before the temperature was increased stepwise ($\Delta T = 25^\circ\text{C}$) to 225°C .

For all adsorption experiments with probe molecules (pyridine, CO, propan-2-ol), the IR spectra reported in the paper are difference spectra obtained after subtraction of the background spectrum.

Catalytic tests: The as-prepared samples (0.02 g diluted in 0.13 g SiC) were fixed with quartz wool in a quartz-tube reactor of 4 mm diameter. The samples were first pretreated in a flow of hydrogen of 20 mL min^{-1} by heating from ambient to 300°C ($10^\circ\text{C min}^{-1}$) then at 300°C for 2 h to activate the sample. Alternatively, the samples were activated in flowing He at 500°C (oxidized ceria). Then, the samples were cooled to reaction temperature in an He flow of 20 mL min^{-1} . For reaction, a flow of helium with 40 mL min^{-1} was saturated with propan-2-ol at 13°C ($p_{\text{propan-2-ol}} = 25\text{ mbar}$) and led over the fixed-bed reactor. The dehydrogenation/dehydration reaction of propan-2-ol was studied in inert atmosphere in the temperature range from 150 to 225°C with steps of 25°C . Every reaction temperature was tested for 80 min. Unconverted propan-2-ol and dehydrogenation/dehydration products were analyzed by gas chromatography on a Hewlett Packard 5890 (Series II) GC equipped with a flame ionization detector. The various components were separated on a Q-column.

Results

Characterization: The specific surface areas of the commercial ceria supported samples were found to be $5\text{--}6\text{ m}^2\text{ g}^{-1}$. The final gold loadings were close to the nominal contents (see Table 1).

The particle size distribution was determined by TEM. Size and dispersion were identified, however, only for the

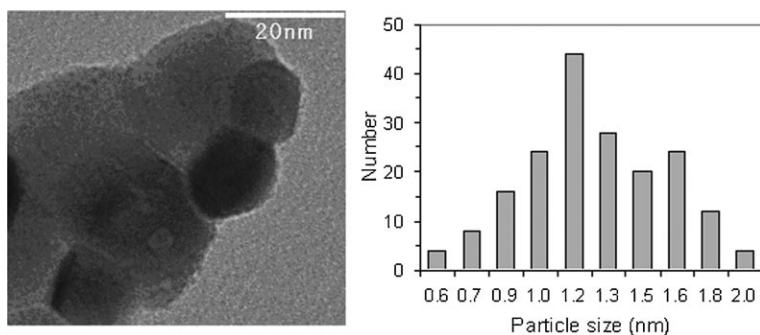


Figure 1. TEM image and particle size distribution of Au/CeO₂(1.0).

sample with the highest Au loading. Determination of the particle size distribution was based on 150 particles. The nanosized particles were well dispersed on the ceria surface (see Figure 1). The main average particle size for Au/CeO₂(1.0) was 1.4 nm.

X-ray diffractograms of ceria (oxidized and reduced) and reduced Au/CeO₂(1.0) samples are shown in Figure 2. Reflections at $2\theta = 28.6, 33.1, 47.5, 56.4, 59.1,$ and 69.5° correspond to cubic fluorite-type ceria. The characteristic reflection of crystalline Au at $2\theta = 38^\circ$ was not observed, which is consistent with the presence of the very small gold particles detected by TEM. Changes of the ceria phase after gold deposition have not been detected.

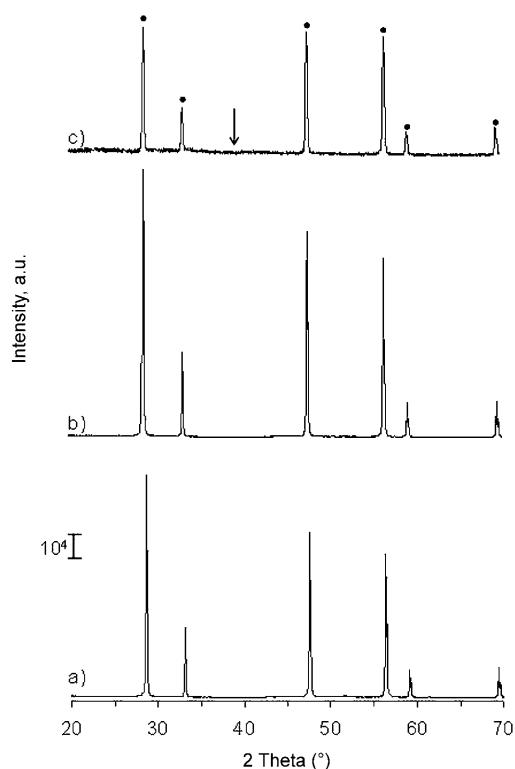


Figure 2. X-ray diffractograms of a) oxidized ceria, b) reduced ceria, and c) Au/CeO₂(1.0) (pretreated in H₂ at 300 °C) (↓ Au diffraction peaks; ● ceria fluorite diffraction peaks).

Infrared spectroscopy with adsorbed pyridine:

Pyridine adsorption on oxidized and reduced ceria surfaces was carried out to identify the nature of acid sites. While for oxidized ceria mainly Ce⁴⁺ is expected, for reduced ceria Ce³⁺ was expected to be the dominant species. Before pyridine was adsorbed at 0.1 mbar and 50 °C, the pretreated samples were activated in situ in vacuum at

300 °C to remove carbonates and water. Well-resolved bands were obtained after subtraction of the background (spectrum of the activated sample) for all samples. The relevant part of the spectra between 1650 and 1400 cm⁻¹ is shown in Figure 3.

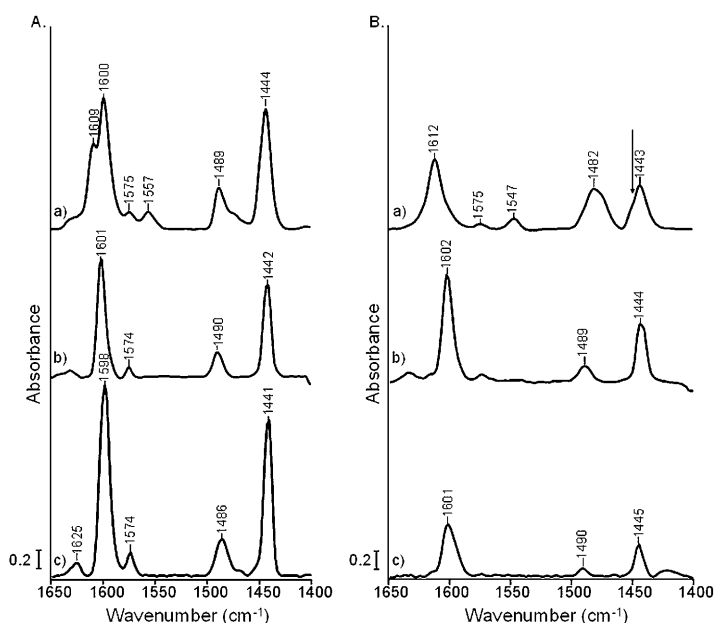


Figure 3. IR difference spectra obtained after pyridine adsorption at 50 °C (A) and after evacuation at 200 °C for one hour (B). a) Oxidized ceria; b) reduced ceria; c) Au/CeO₂(1.0). The samples were activated in vacuum at 300 °C after the respective pretreatment (oxidation, reduction).

For oxidized ceria, the bands of pyridine ring vibrations appeared at 1444 (ν_{19b}), 1489 (ν_{19a}), 1575 (ν_{8b}), and 1600/1628 cm⁻¹ (ν_{8a}). The occurrence of the ν_{8a} band at two different wavenumbers was ascribed by Zaki et al.^[1] to Lewis acid sites with different strength. The large width at half-height of the band at 1443 cm⁻¹ after evacuation suggests that indeed this band is composed of two contributions (see arrow in spectrum a in Figure 3B). The band at 1557 cm⁻¹ is tentatively attributed to pyridinium ions (pyridine chemisor-

bed at Brønsted acid sites), though this band is usually observed at somewhat lower wavenumbers.^[31]

On reduced ceria, the formation of a band characteristic of pyridinium ions was not observed. Only bands of pyridine coordinatively adsorbed on Lewis acid sites were noted. In comparison to oxidized ceria, the ν_{19b} and ν_{8a} bands were shifted to lower wavenumbers, indicating lower acid-site strength. The shoulder at the ν_{8a} band (1601 cm^{-1}) was not observed. We speculate that after reduction of ceria in hydrogen the largest fraction of accessible Ce^{4+} cations was reduced to Ce^{3+} , so that the remaining bands after pyridine adsorption at 1630 , 1601 , 1490 , and 1442 cm^{-1} can be assigned to Ce^{3+} in different coordination states. The width at half-height of the band at 1444 cm^{-1} was much smaller in this sample after evacuation.

Weakly bound and physisorbed pyridine was removed after evacuation at 200°C . While the intensity of the ν_{19a} band at 1490 cm^{-1} decreased drastically for reduced ceria, it remained with distinct intensity in the case of oxidized ceria. Thus, the rather strong acidity of the latter sample is confirmed. The downshift of the ν_{8a} band from 1612 cm^{-1} for oxidized ceria to 1602 cm^{-1} for reduced ceria emphasizes clearly the lower Lewis acid strength of Ce^{3+} compared to Ce^{4+} induced by reduction in H_2 .

For reduced Au/CeO_2 similar IR spectra as for reduced ceria were obtained after pyridine adsorption. Bands of adsorbed pyridine were found at 1441 , 1486 , 1573 , 1598 , and 1625 cm^{-1} . All bands are attributed to pyridine coordinated to Lewis acid sites. Subtle shifts in the wavenumbers, such as from 1442 to 1441 cm^{-1} for the ν_{19b} band and from 1601 to 1598 cm^{-1} for the ν_{8a} band, indicate weakly bound, that is, mainly physisorbed pyridine.^[32] After heating to 200°C under reduced pressure the same bands as for reduced ceria remained, indicating the dominance of Ce^{3+} for this sample.

Infrared spectroscopy of adsorbed CO: Lewis acid sites were additionally characterized by adsorption of CO on reduced Au/CeO_2 at liquid-nitrogen temperature) followed by IR spectroscopy. Figure 4 shows the difference spectra after adsorption of CO at different pressures for $\text{Au}/\text{CeO}_2(1.0)$. Introduction of successive small volumes of CO at low pressure in pulses led first to the appearance of a band at 2100 cm^{-1} , which is assigned to CO adsorbed on metallic gold (Au^0).^[33,34] Another band of low intensity was also observed at 2170 cm^{-1} . With increasing CO pressure, the bands at 2100 and 2170 cm^{-1} increased in intensity and shifted towards lower wavenumbers (2092 and 2160 cm^{-1}). A third band (2150 cm^{-1}) visible first as a shoulder of the high-wavenumber band, grew gradually in intensity and became the most intense band at high CO pressures. The two bands at high wavenumbers are attributed to CO stretching vibrations of CO linearly adsorbed on surface metal cations.^[35,36,37,38] In accordance with literature, the band at high wavenumber (2170 cm^{-1}) is assigned to CO coordinated to weak Lewis acid sites such as Ce^{3+} ions.^[39,40,41] However, we cannot rule out minor contributions to these bands resulting from CO adsorption on Au^+ (exposed at a shoulder around

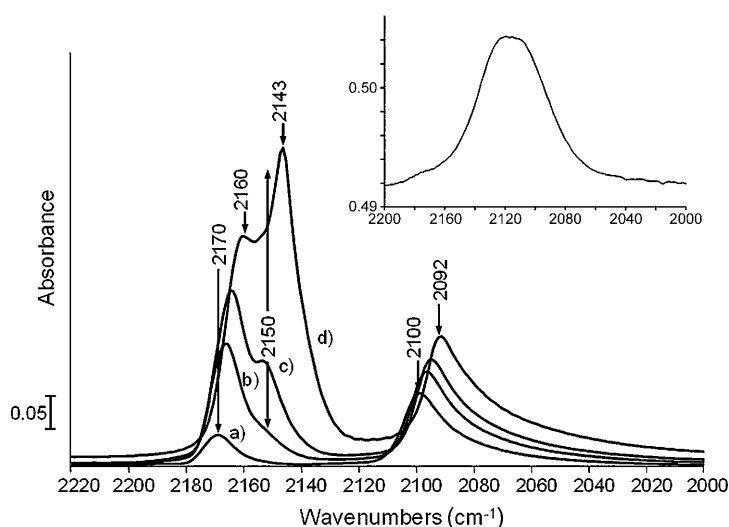


Figure 4. IR difference spectra after CO adsorption at -170°C on $\text{Au}/\text{CeO}_2(1.0)$ activated under H_2 at 300°C . Inset: IR spectrum of $\text{Au}/\text{CeO}_2(1.0)$ after activation in H_2 at 300°C . a) 4×10^{-7} mol (CO); b) 13×10^{-7} mol (CO); c) 22×10^{-7} mol (CO); d) 1.1 mbar (eq. CO)

2150 cm^{-1}).^[40,41] The low-wavenumber band (2150 – 2043 cm^{-1}) shifting to lower wavenumbers with increasing pressure is assigned to physisorbed CO.^[23,42] Note that the IR spectrum (insert Figure 4) recorded after reductive activation of Au/CeO_2 showed a band at 2120 cm^{-1} characteristic of the forbidden transition of Ce^{3+} .^[43]

The experiment performed with $\text{Au}/\text{CeO}_2(0.1)$ (not shown) exhibited similar bands at identical wavenumbers and intensities to those observed with $\text{Au}/\text{CeO}_2(1.0)$, except for the band at 2090 cm^{-1} , which was very weak because of the very low gold loading. This experiment strongly indicates that the high-wavenumber bands located at 2170 and 2150 cm^{-1} are to be assigned to CO adsorbed on Ce^{3+} and Ce^{4+} , as well as physisorbed CO. The band at 2100 – 2092 cm^{-1} is attributed to Au^0 , while the presence of contributions from Au^+ would be masked by the stronger contributions from CO adsorbed on Ce cations and from physisorbed CO.

Adsorption of CO also induces changes in the high-wavenumber range of the spectrum of $\text{Au}/\text{CeO}_2(1.0)$ corresponding to OH vibrations (Figure 5). Three OH bands were initially observed at 3722 , 3678 , and 3637 cm^{-1} (Figure 5, curve a) while the band at 3450 cm^{-1} was hardly observed. Note, that the wavenumbers are shifted compared to those observed in Figure 4. This arises from the lower temperature at which the spectrum was recorded and underlines the anharmonicity of the vibrations. The band at 3722 cm^{-1} is assigned to OH groups coordinated to one metal cation.^[35,44] The two bands at 3678 and 3637 cm^{-1} are assigned to two types of doubly bridging OH groups,^[45] while a broad band at 3450 cm^{-1} (hardly observed in the present case) is usually assigned to triply bridging OH species^[46] or to hydrogen-bonded OH groups.^[45,47] The intensities of the bands at 3722 , 3678 , and 3637 cm^{-1} decreased markedly when CO

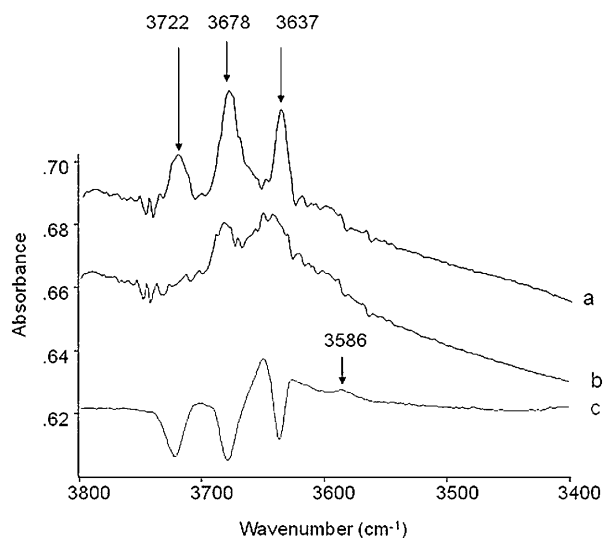


Figure 5. IR spectra of Au/CeO₂(1.0) a) after activation in H₂ at 300 °C and b) after adsorption of CO (1 Torr eq.); c) difference spectrum (b–a).

was introduced (Figure 5, curve b), and at least two new bands appeared at 3586 and 3650 cm⁻¹. Both are more visible in the difference spectrum (Figure 5, curve c). They arise from OH vibrations perturbed by CO adsorbed on OH. The band at 3637 cm⁻¹ is downward-shifted by around 50 cm⁻¹ (band at 3586 cm⁻¹), which is a small shift compared to that of 300 cm⁻¹ observed, for instance, in acidic zeolite and indicates a lower acid strength of ceria.

Infrared spectroscopy during propan-2-ol conversion: Conversion of propan-2-ol was also followed by in situ IR spectroscopy. The samples were oxidized in synthetic air or reduced in H₂ at 300 °C before passing a helium/propan-2-ol flow over them. Under these conditions, propene and acetone may be formed from propan-2-ol over acid or basic sites, respectively. Figure 6 shows the difference spectra on admission of propan-2-ol on oxidized ceria at 225 °C (curve a), reduced ceria (curve b), and reduced Au/CeO₂(1.0) (curve c), that is, the IR spectra after that procedure minus the IR spectra after activation.

Let us first address evidence that propan-2-ol was adsorbed dissociatively. Two weak bands characteristic of cerium alkoxides were observed at 1157 and 1114 cm⁻¹ on oxidized ceria. The cerium alkoxide bands are shifted to lower wavenumbers (1153/1101 cm⁻¹) on reduced ceria, which is in agreement with the lower acid-site strength of cerium cations. On adding Au to ceria, the adsorption bands of cerium alkoxide were observed at 1158/1131 cm⁻¹. Therefore, propan-2-ol was concluded to be dissociatively adsorbed on all samples.^[47]

Three bands in the C–H stretching region were found at 2963, 2929, and 2851 cm⁻¹ for oxidized ceria. These bands together with bands around 1157/1114 cm⁻¹ are characteristic of isopropoxyl groups.^[26] In case of reduced ceria similar bands were observed, but slightly shifted to higher wavenumbers (2979, 2933, 2898 cm⁻¹). In the presence of Au, these bands

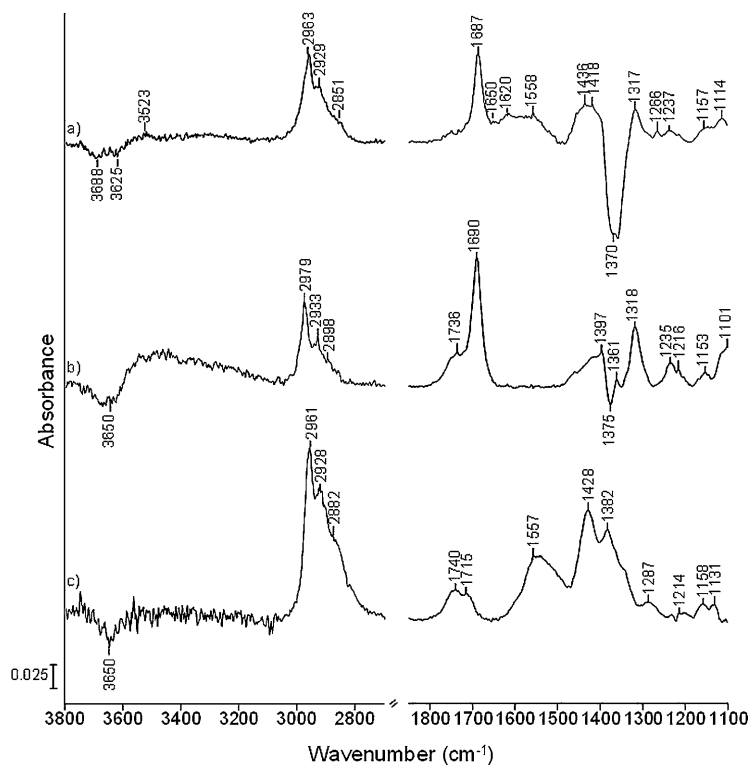


Figure 6. IR difference spectra of ceria and Au/CeO₂(1.0) in the presence of a flow of 25 mbar propan-2-ol in He at 225 °C after one hour time on stream. a) Oxidized ceria; b) reduced ceria; c) Au/CeO₂(1.0).

were observed at 2961, 2928, and 2882 cm⁻¹ and are more likely associated with adsorbed acetone or acetone precursors (see below) than with isopropoxyl groups.

Characteristic carbonyl bands between 1750 and 1200 cm⁻¹ were observed for all samples (see Figures 6 and 7), and support the existence of acetone precursors and/or acetone coordinated to relatively strong Lewis acid sites together with bands of carboxylates (1500 cm⁻¹) and hydroxycarbonates or carbonates (ca. 1300 cm⁻¹). In detail, the difference spectra of ceria and Au loaded ceria varied markedly in the range of 1680–1750 cm⁻¹, indicating formation of various surface precursors (see Figure 6). For oxidized ceria, a band was observed at 1687 cm⁻¹ indicating the presence of an acetone precursor. Note that the νC=O band of weakly coordinated acetone appears between 1720 and 1710 cm⁻¹ on moderately Lewis acidic oxides.^[48] A small band at 1620 cm⁻¹ is attributed to the νC=C stretching band and indicates formation of propene by dehydration of propan-2-ol.^[49] The broad band at approximately 3500 cm⁻¹ suggests the presence of hydrogen-bonded OH groups or of bound water molecules.

After reduction of ceria, the carbonyl band of the adsorbed acetone precursor shifted to 1690 cm⁻¹. Furthermore, a distinct shoulder appeared at 1736 cm⁻¹, which is attributed to acetone with a very weakly coordinating C=O group. In the case of reduced Au/CeO₂(1.0), two bands were observed at 1740 and 1715 cm⁻¹, attributed to two types of weakly adsorbed acetone. The band at 1620 cm⁻¹ character-

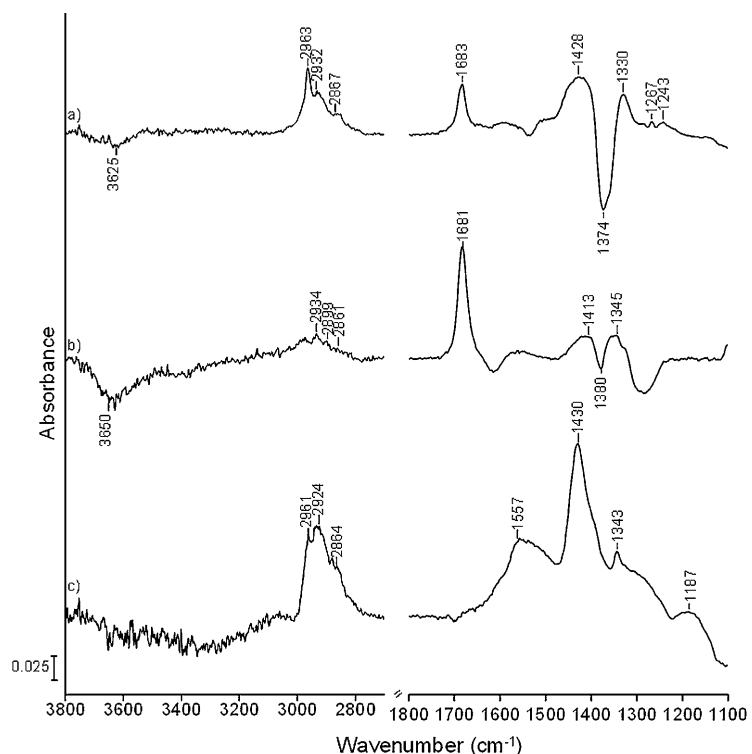


Figure 7. IR difference spectra of ceria and Au/CeO₂(1.0) samples after flushing in He-flow at 225 °C exposing the samples before to a flow of 25 mbar propan-2-ol in He for one hour. a) Oxidized ceria; b) reduced ceria; c) Au/CeO₂(1.0).

istic of propene was neither observed with reduced ceria nor with Au/CeO₂(1.0).

The interaction of propan-2-ol (undissociated) with hydroxyl groups of oxidized and reduced ceria caused a negative band around 3650 cm⁻¹ associated with the appearance of a broad weak band around 3500 cm⁻¹ (Figure 6a and b). These changes come together with the strong negative band at 1370 cm⁻¹ attributed to the interaction of propan-2-ol with hydroxycarbonates (C=O hydroxycarbonates: 1317–1230 cm⁻¹).^[50] The intensity variation of the band at 1370 cm⁻¹ is much stronger for oxidized than for reduced ceria, whereas the broad weak band around 3500 cm⁻¹ is stronger for reduced ceria.

After flushing the oxidized ceria sample with helium at 225 °C, the negative band at

3688 cm⁻¹ disappeared, indicating the removal of physisorbed propan-2-ol (see Figure 7, curve a). At the same time, the bands at 3625 (negative), 1683 (positive), and 1374 cm⁻¹ (negative) were still observed, suggesting that the chemisorbed propan-2-ol intermediate still interacts with surface hydroxycarbonates. With further temperature increase to 300 °C, the remaining carbonyl band at 1683 cm⁻¹ almost disappeared, while the negative bands hardly changed (see Figure 8, curve a). This indicates that part of the hydroxycarbonate must have also eliminated water and transformed into bidentate carbonates.

On flushing reduced ceria with helium at 225 °C (Figure 7b), a carbonyl band located at 1681 cm⁻¹ remained with distinct intensity together with two negative bands at 3650 and 1380 cm⁻¹ indicating relatively strong adsorption of the acetone precursor. Raising the temperature to 300 °C caused a distinct decrease of this carbonyl band and formation of carbonates (1399–1229 cm⁻¹, Figure 8b).

Treating Au/CeO₂(1.0) with propan-2-ol at 225 °C causes no variations of the intensity of the (negative) C=O bands characteristic of hydroxycarbonates at 1370 cm⁻¹ (Figure 6c), but two strong bands appeared at 1557 and 1428 cm⁻¹ and are attributed to surface carboxyl groups.^[51] A smaller band at 1382 cm⁻¹ is attributed to C–H vibrations of the methyl groups of these carboxylate species or to adsorbed acetone.^[49]

On flushing reduced ceria with He, a carbonyl band located at 1681 cm⁻¹ remained with distinct intensity together with two negative bands at 3650 and 1380 cm⁻¹ indicating

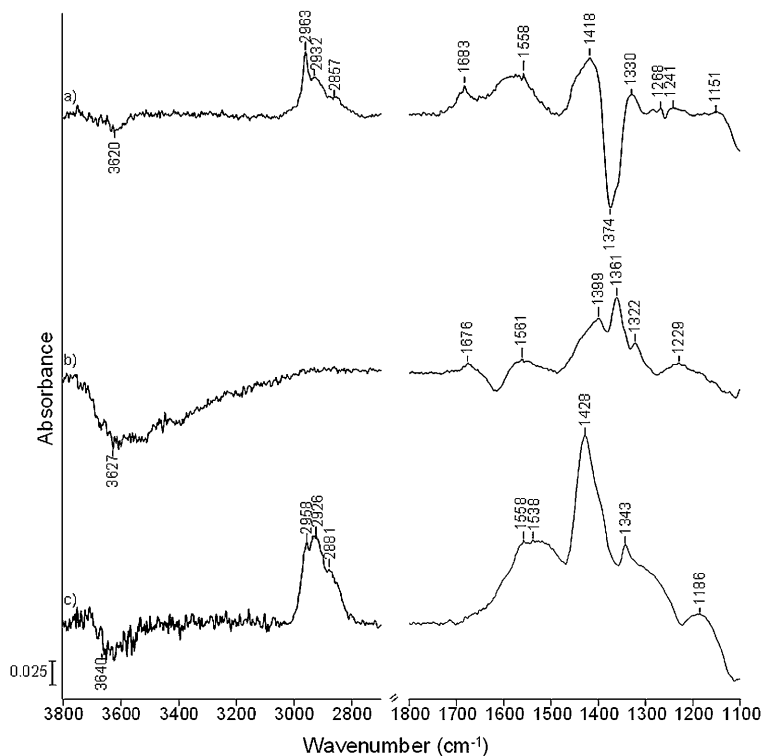


Figure 8. IR difference spectra of ceria and Au/CeO₂(1.0) samples obtained after desorbing propan-2-ol at 300 °C in He-flow. a) Oxidized ceria; b) reduced ceria; c) Au/CeO₂(1.0).

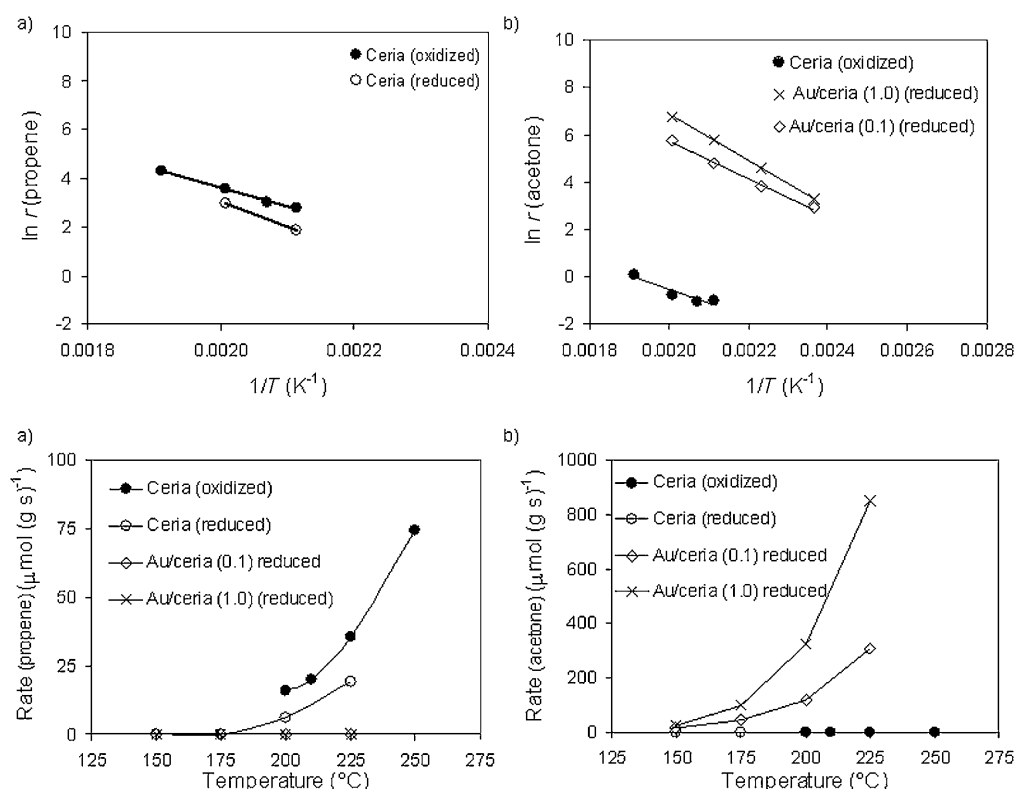


Figure 9. Arrhenius plots and rates of product formation for propan-2-ol conversion from 150 to 250 °C for various pretreated ceria and Au/CeO₂ samples. a) Formation of propene; b) formation of acetone.

relatively strong adsorption of the acetone precursor. Raising the temperature to 300 °C caused a distinct decrease of this carbonyl band and the formation of carbonates (1399–1229 cm⁻¹) on reduced ceria. In contrast, three bands in the νC–H vibration region remained in case of Au/CeO₂(1.0). The carbonyl bands associated with weakly adsorbed acetone at 1740 and 1715 cm⁻¹ were removed after switching to pure He flow.

Catalytic conversion of propan-2-ol: The rates of formation of propene and acetone for all investigated samples are summarized in Figure 9. At temperatures below 200 °C, propan-2-ol conversion was not observed for oxidized ceria. At 200 °C, propene was formed with a rate of 16 μmol g⁻¹ s⁻¹ (6% conversion) and 98% selectivity. After increasing the temperature to 225 °C, conversion almost doubled to 35 μmol g⁻¹ s⁻¹ (14%) with 99% selectivity to propene. Oxidized ceria underwent 21% deactivation at 225 °C during 80 min of propan-2-ol reaction.

For reduced ceria, the rate of propan-2-ol dehydration at 200 °C was 6 μmol g⁻¹ s⁻¹ (0.3% conversion), and propene was formed with 100% selectivity. Propene was still formed with 100% selectivity at 225 °C, but again only with low activity (19 μmol g⁻¹ s⁻¹, 0.6% conversion). Reduced ceria underwent 25% deactivation at 225 °C during 80 min of propan-2-ol reaction.

For the reduced Au/CeO₂(0.1) sample, conversion of propan-2-ol was observed already at 150 °C. At all investigated temperatures solely acetone was formed. The activity increased from 18 μmol g⁻¹ s⁻¹ (1% conversion) at 150 °C to 308 μmol g⁻¹ s⁻¹ (10% conversion) at 225 °C.

For the reduced Au/CeO₂(1.0) sample, conversion of propan-2-ol was also observed already at 150 °C. At all investigated temperatures solely acetone was formed. The activity increased from 26 μmol g⁻¹ s⁻¹ (1% conversion) at 150 °C to 847 μmol g⁻¹ s⁻¹ (28% conversion) at 225 °C. In contrast to ceria, Au/CeO₂(1.0) showed stable catalytic activity even at the highest reaction temperatures.

While the rate of dehydration was 35 μmol g⁻¹ s⁻¹ with oxidized ceria and 19 μmol g⁻¹ s⁻¹ with reduced ceria (at 225 °C), the deposition of even the smallest concentration of gold on ceria suppressed the formation of propene. While for pure ceria the rates of dehydrogenation were hardly measurable (<0.5 μmol g⁻¹ s⁻¹) at 225 °C, they were dramatically higher for the Au/CeO₂ catalysts; for example, the rates increased with increasing concentration of Au from 308 to 847 μmol g⁻¹ s⁻¹ for 0.1 and 1.0 wt % Au at 225 °C.

The apparent activation energies (see Arrhenius plots in Figure 9) for dehydration were determined to 65 and 87 kJ mol⁻¹ for oxidized and reduced ceria, respectively. The apparent activation energy for dehydration of acetone was 47 kJ mol⁻¹ for oxidized ceria, 66 kJ mol⁻¹ for Au/CeO₂(0.1), and 81 kJ mol⁻¹ for Au/CeO₂(1.0).

Discussion

Pure CeO₂ is generally described as a moderately strong solid acid.^[2] Accordingly, IR spectroscopy on adsorbed pyridine indicates the presence of different types of Lewis acid sites and, only in case of oxidized ceria, of a low concentration of Brønsted acid sites. In consequence, after evacuation of oxidized ceria at 200 °C bands at 1443 and 1547 cm⁻¹ are assigned to pyridine coordinated to Lewis acid sites of moderate strength (i.e., Ce⁴⁺ and Ce³⁺) and to Brønsted acid sites, respectively. The minor shoulder in the peak at 1443 cm⁻¹ at higher wavenumber is tentatively attributed to pyridine adsorbed on Ce⁴⁺, and hence the main band (Figure 3 a) to pyridine adsorbed on Ce³⁺.

The nature and concentration of acid sites was changed by the reduction of ceria. The lack of the characteristic bands of pyridinium ions indicates the absence of Brønsted acid sites. Compared to oxidized ceria, the lower wavenumber of the ν_{8a} band (1602 cm⁻¹) indicates that the strength of Lewis acid sites was much lower. Thus, we conclude that at least a major fraction of the coordinatively unsaturated Ce⁴⁺ was reduced to Ce³⁺. Note that the shoulder at the band at 1444 cm⁻¹ indeed has lost drastically in intensity, and the overall band has become narrower. This tendency was even more pronounced with Au/CeO₂(1.0), as not only pyridine adsorbed on the stronger Lewis acidic Ce⁴⁺ disappeared, but also the concentration of accessible Ce³⁺ decreased after reduction in the presence of Au.

Besides supporting these interpretations, the IR spectra of adsorbed CO on Au/CeO₂(1.0) also provide information on the nature of the Au species. A band assigned to the forbidden transition of Ce³⁺ at 2120 cm⁻¹ appeared in the spectrum of Au/CeO₂(1.0) after activation in hydrogen at 300 °C (see inset in Figure 4).^[44] The sites binding CO the strongest (2170 and 2100 cm⁻¹) are attributed to adsorption of CO on Ce³⁺ and on Au⁰. The latter assignment is derived by comparison with different Au loadings on CeO₂.

With increasing coverage, a small band and later shoulder is found at 2150 cm⁻¹ attributed to CO adsorption on Au⁺ species acting as relatively weak and soft Lewis acid sites. The intense band at 2150–2140 cm⁻¹ is characteristic for adsorption of CO on OH groups. The band at 2100 cm⁻¹ increased continuously with increasing surface coverage and partial pressure and led us to conclude that the main fraction of accessible Au is in the metallic state. The fact that the maximum of the band shifts to lower wavenumbers is puzzling, as it indicates that sites of increasing backdonation to CO are occupied. It is unclear at present, however, whether this effect is induced by the adsorbed CO or the Au particles rearrange in the presence of CO.^[52]

The IR spectra of adsorbed propan-2-ol show important changes of the sites at the ceria surface induced by reduction in hydrogen and by deposition of Au particles. On all materials acetone or the surface precursor of acetone is formed ($\bar{\nu}_{C=O} = 1687$ cm⁻¹). The presence of this band (after exposing oxidized CeO₂ to propan-2-ol at 225 °C) is accompanied by the appearance of OH stretching bands around

3500 cm⁻¹ in the form of a relatively broad and structured feature in the difference spectrum (IR spectrum of CeO₂ after that procedure minus the IR spectrum of the activated CeO₂), as well as by two negative bands at 3625 and 1370 cm⁻¹ (see Figure 6a) These two bands are identified as characteristic of surface hydroxycarbonates (OH and C=O vibrations).^[36] This is in accordance with the fact that the thermal decomposition of cerium carbonate in He or H₂ starts at 190 °C and is completed at 500 °C.^[53,54] Adsorption of propan-2-ol occurs with the simultaneous appearance of OH stretching bands associated with ceria and a decrease in the concentration of surface hydroxycarbonates. We speculate that the appearance of the OH band at 3500 cm⁻¹ accompanied by formation of an adsorption band at 1650 and 1620 cm⁻¹ indicates that propan-2-ol is dehydrated to propene and that water and propene are adsorbed to some extent.^[26]

Acetone interacts as electron-pair donor with the Lewis acid sites (electron-pair acceptor sites) of metal oxides. The strength of this interaction increases with increasing Lewis acidity of the site, and as a result the lower the wavenumber the C=O group will be. Thus, the C=O band observed at 1687 cm⁻¹ in the case of oxidized ceria (presence of Ce⁴⁺) indicates the strongest interaction with the C=O group. A shift to 1736 cm⁻¹ was observed in the case of reduced ceria (Ce³⁺). Consequently, for Au/ceria the band observed at 1740 cm⁻¹ can be attributed to very weak Lewis acid sites such as Ce³⁺ or Au⁺ ions, whereas that at 1715 cm⁻¹ is attributed to Ce³⁺ at the Au/ceria interface having a slightly higher Lewis acid strength.

The presence of the band at 1687 cm⁻¹ suggests that the C–O bond of chemisorbed propan-2-ol resembles more a keto group than an alcoholate. The simultaneous disappearance of vibrations of hydroxycarbonates (3625 and 1370 cm⁻¹) led us to speculate that the OH group in the hydroxycarbonate interacts with the carbon atom of this moiety (see Figure 6). It is remarkable that this complex interaction seems to be reversible for propan-2-ol, as further increase of the temperature under He flow led to desorption of propan-2-ol (Figure 7a). If the evacuation temperature was raised to 300 °C, the intensity of the band at 1683 cm⁻¹ remaining was marginal, but the concentration of hydroxyl carbonate (3620 cm⁻¹) has still been reduced compared to the situation before the adsorption of propan-2-ol (see Figure 8a). This suggests that the decrease in intensity of the bands of hydroxycarbonate stems not only from the reversible interaction with surface bound propan-2-ol, but also from conversion from a hydroxycarbonate to a bidentate carbonate. This conclusion is supported by the fact that the bands of hydroxycarbonate do not reappear after desorption of propan-2-ol, that is, the corresponding negative band does not lose intensity despite desorption of all surface species derived from propan-2-ol.

The higher intensity of the band at 1690 cm⁻¹ with reduced CeO₂ at 225 °C suggests that the concentration of the precursor to acetone or adsorbed acetone is higher than in the case of oxidized ceria, that is, these species are formed to a more significant extent.

The relatively high frequency of the C=O vibrations at 1740/1715 cm^{-1} for Au/CeO₂(1.0) indicates that the interaction of acetone with the catalyst surface is relatively weak. Note that, despite the tenfold higher conversion of propan-2-ol to acetone in the catalytic flow experiment, the surface coverage by acetone or its precursor is quite low, in line with the weak interaction between acetone and the catalyst surface.

Overall, dehydrogenation of propan-2-ol is initialized by dissociative adsorption of the alcohol on an acid–base site, that is, on exposed Ce³⁺/Ce⁴⁺ and oxygen surface atoms. This is supported by the fact that bands characteristic of cerium alkoxide (1158/1114 cm^{-1}) are observed for all samples in the situ IR experiments. The low intensity of these bands points to low surface concentrations of these species. However, the results also suggest that the interaction of propan-2-ol varies between oxidized and reduced ceria as well as with Au/CeO₂(1.0). Under reaction conditions, the interaction of propan-2-ol with surface OH groups only resulted in a negative band near 3650 cm^{-1} in the case of reduced ceria and Au/CeO₂(1.0), hardly providing evidence for the formation of new OH bands (Figure 6c). In contrast, the band at 3500 cm^{-1} appearing in the case of oxidized and reduced ceria indicates formation of hydrogen-bonded OH groups (from which water may be formed) during the dehydration of propan-2-ol to propene. Formation of carbonates (1318–1235 cm^{-1}), which was observed for both ceria samples, was markedly less pronounced in the presence of Au.

The type of catalytic elimination from propan-2-ol (see Figure 10) changes from elimination of water (100% selectivity to propene) for CeO₂ to dehydrogenation (100% selectivity to acetone) for Au/CeO₂ samples. During the conversion of propan-2-ol with ceria, the catalysts were markedly deactivated (>20%) with time on stream, while the Au/CeO₂ catalysts were extremely stable.

Combining the acid–base characterization and the surface chemistry of propan-2-ol, the high selectivity towards ace-

tone for Au/CeO₂ is attributed to the transformation of Ce⁴⁺ to Ce³⁺ or the blocking of Ce⁴⁺. This demonstrates clearly that the reaction path to propene via dehydration of propan-2-ol requires the presence of strong Ce⁴⁺ cations. The rate of dehydrogenation, in contrast, is related to the concentration of Au. We tentatively conclude at present that the formation of Au⁺ on the Au/CeO₂ interface creates very weak and soft Lewis acid sites, which enhance hydride abstraction. This strongly facilitates the last step in the catalytic dehydrogenation. At the same time, elimination of Ce⁴⁺ and the presence of Au reduces the retention of acetone by decreasing the formation of carboxylates and thus stabilizing the catalytic activity. These carboxylates form from adsorbed acetone on most basic mixed oxides and are characterized by IR bands observed at 1557 and 1428 cm^{-1} attributed to asymmetric and symmetric νCOO^- vibrations, respectively.^[48]

Conclusion

Deposition–precipitation of Au on a CeO₂ support modifies the surface by in situ formation of Ce³⁺ and Au⁺ at the Au/CeO₂ interface. We conclude that Au interacts selectively with Ce⁴⁺ to eliminate its accessibility and function as a strong Lewis acid. Simultaneously, it induces formation of very soft Lewis acid sites, presumably by generation of Au⁺ at the Au/CeO₂ interface. The latter site facilitates hydride abstraction.

The combination of these effects leads to suppression of the dehydration of propan-2-ol that dominates with the parent oxidized CeO₂. This reaction route is induced by strong interaction of the oxygen atom of propan-2-ol with Ce⁴⁺ and the presumably simultaneous elimination of a proton at the β -carbon atom. Reduction of CeO₂ lowers the rate of dehydration by reducing the concentration of Ce⁴⁺, but it does not eliminate this reaction pathway completely. The presence of a high concentration of Ce³⁺ alone, however, is apparently not able to catalyze the dehydrogenation of propan-2-ol. On the surface, acetone or its precursor is formed, but irreversibly bound to the CeO₂ surface under a wide variety of operating conditions.

The presence of Au eliminates the deactivation of CeO₂ associated with the presence of at least moderately strong and relatively hard Ce⁴⁺ Lewis acid sites. Only dehydrogenation of propan-2-ol is catalyzed, and the dehydration pathway is completely blocked. In this reaction pathway, the alcohol is dissociatively adsorbed, forming an alkoxy species at Ce³⁺ and a hydroxyl group. As the rate of dehydrogenation increases with increasing concentration of Au and the main path of dehydrogenation of propan-2-ol on the Au particles can be ruled out (low activity for catalyzing the reverse reaction), we suggest that the Au particles provide weak and extremely soft Lewis acid sites at the support/metal interface that facilitate the acceptance of hydride ions and thus accelerate dehydrogenation.

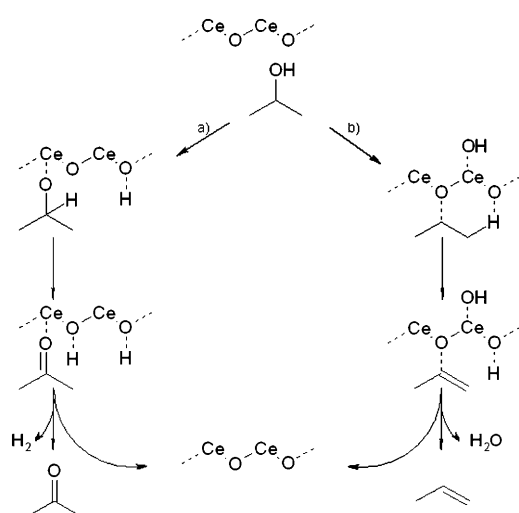


Figure 10. Schematic mechanism of propan-2-ol adsorption on ceria. a) Formation of acetone over isopropoxide intermediate; b) formation of propene over carbenium-ion intermediate.

The interplay of selective deposition of Au and subtle modification of the support has thus led to a uniquely basic material. The results show indeed that the leads from DFT calculations and UHV investigations on CeO₂ (111) model systems could be successfully translated to high surface area catalyst systems.

Acknowledgements

We are grateful to Dr. Laurent Delannoy (LRS) for helpful discussions as well as to Dr. Katia Fajerberg, who initiated the collaboration. We are grateful to Mrs. Monika Pop for performing the catalysis experiments.

- [1] M. I. Zaki, G. A. M. Hussein, S. A. A. Mansour, H. E. El-Ammawy, *J. Mol. Catal.* **1989**, *51*, 209.
- [2] A. Trovarelli, *Catal. Rev. Sci. Eng.* **1996**, *38*, 439.
- [3] E. Iglesia, D. G. Barton, J. A. Biscardi, M. J. L. Gines, S. L. Soled, *Catal. Today* **1997**, *38*, 339.
- [4] V. Matolin, M. Cabala, I. Matolinova, M. Skoda, J. Libra, M. Vaclavu, K. C. Prince, T. Skala, H. Yoshikawa, Y. Yamashita, S. Ueda, K. Kobayashi, *J. Phys. D* **2009**, *42*, 115301.
- [5] G. C. Bond, D. T. Thompson, *Catal. Rev. Sci. Eng.* **1999**, *41*, 319.
- [6] F. Marino, C. Descorme, D. Duprez, *Appl. Catal. B* **2004**, *54*, 59.
- [7] C. Milone, R. Ingoglia, L. Schipilliti, C. Crisafulli, G. Neri, S. Galvagno, *J. Catal.* **2005**, *236*, 80.
- [8] A. Corma, P. Serna, *Science* **2006**, *313*, 332.
- [9] A. Ueda, M. Haruta, *Gold Bull.* **1999**, *32*, 3.
- [10] T. Bunluesin, R. J. Gorte, G. W. Graham, *Appl. Catal. B* **1998**, *15*, 107.
- [11] W. Deng, J. D. Jesus, H. Saltsburg, M. Flytzani-Stephanopoulos, *Appl. Catal. A* **2005**, *291*, 126.
- [12] Q. Fu, A. Weber, M. Flytzani-Stephanopoulos, *Catal. Lett.* **2001**, *77*, 87.
- [13] H. Daly, J. Ni, D. Thompsett, F. X. Meunier, *J. Catal.* **2008**, *254*, 238.
- [14] A. Sandoval, A. Gomez-Cortes, R. Zanella, G. Diaz, J. M. Saniger, *J. Mol. Catal. A Chem.* **2007**, *278*, 200.
- [15] M. Haruta, S. Tsubota, T. Kobayashi, H. Kageyama, M. J. Genet, B. Delmon, *J. Catal.* **1993**, *144*, 175.
- [16] J. T. Miller, A. J. Kropf, Y. Zha, J. R. Regalbuto, L. Delannoy, C. Louis, E. Bus, J. A. van Bokhoven, *J. Catal.* **2006**, *240*, 222.
- [17] I. N. Remediakis, N. Lopez, J. K. Norskov, *Angew. Chem.* **2005**, *117*, 1858; *Angew. Chem. Int. Ed.* **2005**, *44*, 1824.
- [18] J. Meilin, B. Haifeng, S. Yuenain, L. Yanfeng, *J. Rare Earth* **2008**, *26*, 538.
- [19] L. Delannoy, N. Weiher, N. Tsapatsaris, A. M. Beesley, L. Nchari, S. L. M. Schroeder, C. Louis, *Top. Catal.* **2007**, *44*, 263.
- [20] L. Ilieva, J. W. Sobczak, M. Manzoli, B. L. Su, D. Andreeva, *Appl. Catal. A* **2005**, *291*, 85.
- [21] N. Weiher, E. Bus, L. Delannoy, C. Louis, D. E. Ramaker, J. T. Miller, J. A. van Bokhoven, *J. Catal.* **2006**, *240*, 100.
- [22] N. J. Castellani, M. M. Branda, K. M. Neyman, F. Illas, *J. Phys. Chem. C* **2009**, *113*, 4948.
- [23] M. Baron, O. Bondarchuk, D. Stacchiola, S. Shaikhutdinov, H. J. Freund, *J. Phys. Chem. C* **2009**, *113*, 6042.
- [24] J. A. Lercher, C. Gründling, G. Eder-Mirth, *Catal. Today* **1996**, *27*, 353.
- [25] I. Halasz, H. Vinek, K. Thomke, H. Noller, *Z. Phys. Chem. (München Ger.)* **1985**, *144*, 157.
- [26] M. I. Zaki, N. Sheppard, *J. Catal.* **1983**, *80*, 114.
- [27] S. R. Blazzkowski, R. A. vanSanten, *J. Am. Chem. Soc.* **1996**, *118*, 5152.
- [28] A. Gervasini, J. Fenyvesi, A. Auroux, *Catal. Lett.* **1997**, *43*, 219.
- [29] K. C. Waugh, M. Bowker, R. W. Petts, H. D. Vandervell, J. Omalley, *Appl. Catal.* **1986**, *25*, 121.
- [30] D. Haffad, A. Chambellan, J. C. Lavalley, *J. Mol. Catal. A Chem.* **2001**, *168*, 153.
- [31] M. I. Zaki, G. A. M. Hussein, S. A. A. Mansour, H. M. Ismail, G. A. H. Mekhemer, *Colloids Surf. A* **1997**, *127*, 47.
- [32] C. Morterra, G. Cerrato, *Langmuir* **1990**, *6*, 1810.
- [33] H. Idriss, *Platinum Met. Rev.* **2004**, *48*, 105.
- [34] M. Manzoli, F. Boccuzzi, A. Chiorino, F. Vindigni, W. Deng, M. Flytzani-Stephanopoulos, *J. Catal.* **2007**, *245*, 308.
- [35] A. Badri, C. Binet, J.-C. Lavalley, *J. Chem. Soc. Faraday Trans.* **1996**, *92*, 4669.
- [36] C. Binet, M. Daturi, J. C. Lavalley, *Catal. Today* **1999**, *50*, 207.
- [37] M. Daturi, C. Binet, J. C. Lavalley, G. Blanchard, *Surf. Interface Anal.* **2000**, *30*, 273.
- [38] C. Li, Y. Sakata, T. Arai, K. Domen, K. Maruya, T. Onishi, *J. Chem. Soc. Faraday Trans. 1* **1989**, *85*, 929.
- [39] C. Binet, A. Jadi, J. C. Lavalley, *J. Chim. Phys. Phys.-Chim. Biol.* **1992**, *89*, 31.
- [40] M. Maciejewski, P. Fabrizioli, J. D. Grunwaldt, O. S. Beckert, A. Baiker, *Phys. Chem. Chem. Phys.* **2001**, *3*, 3846.
- [41] M. I. Zaki, H. Knözinger, *Spectrochim. Acta A* **1987**, *43*, 1455.
- [42] A. S. Ivanova, B. L. Moroz, E. M. Moroz, Y. V. Larichev, E. A. Paukshtis, V. I. Bukhtiyarov, *J. Solid State Chem.* **2005**, *178*, 3265.
- [43] C. Binet, A. Badri, J. C. Lavalley, *J. Phys. Chem.* **1994**, *98*, 6392.
- [44] C. Li, Y. Sakata, T. Arai, K. Domen, K. I. Maruya, T. Onishi, *J. Chem. Soc. Faraday Trans. 1* **1989**, *85*, 1451.
- [45] F. Menegazzo, M. Manzoli, A. Chiorino, F. Boccuzzi, T. Tabakova, M. Signoretto, F. Pinna, N. Pernicone, *J. Catal.* **2006**, *237*, 431.
- [46] O. Pozdnyakova, D. Teschner, A. Wootsch, J. Krohnert, B. Steinhauer, H. Sauer, L. Toth, F. C. Jentoft, A. Knop-Gericke, Z. Paal, R. Schlögl, *J. Catal.* **2006**, *237*, 1.
- [47] A. Abad, P. Concepcion, A. Corma, H. Garcia, *Angew. Chem.* **2005**, *117*, 4134; *Angew. Chem. Int. Ed.* **2005**, *44*, 4066.
- [48] J. A. Lercher, *Z. Phys. Chem. (München Ger.)* **1982**, *129*, 209.
- [49] L. H. Little, *Infrared Spectra of Adsorbed Species*, Academic Press, New York, **1966**.
- [50] L. J. Bellamy, *The Infrared Spectra of Complex Molecules*, Vol. 2, 2nd ed., Chapman and Hall, **1980**.
- [51] J. A. Lercher, H. Noller and G. Ritter, *J. Chem. Soc. Faraday Trans. 1* **1981**, *77*, 621 (i).
- [52] A. M. Joshi, W. N. Delgass, K. T. Thomson, *J. Phys. Chem. C* **2007**, *111*, 11424.
- [53] C. Padeste, N. W. Cant, D. L. Trimm, *Catal. Lett.* **1994**, *24*, 95–105.
- [54] E. Aneggi, J. Llorca, M. Boaro, A. Trovarelli, *J. Catal.* **2005**, *234*, 88.

Received: July 16, 2010
Revised: February 4, 2011
Published online: May 6, 2011